Tanzania Journal of Science 48(3): 528-536, 2022
ISSN 0856-1761, e-ISSN 2507-7961

Pulsed Lased Deposition of Single-Crystalline (001) Oriented $Pb(Zr_{0.5}T_{0.5})O_3$ Thin Film on $PrScO_3$ Substrate

Mahamudu H Mtebwa[*1] and Nava Setter[2]

[1]*Department of Mechanical and Industrial Engineering, University of Dar es Salaam, P.O. Box 35131, Tanzania*

[2]*School of Engineering, Swiss Federal Institute of Technology of Lausanne, CH-1015 Lausanne, Switzerland*

**Corresponding author, e-mail: mtebwa@udsm.ac.tz; mahamudu.mtebwa@gmail.com*

Received 29 Mar 2022, Revised 9 Aug 2022, Accepted 15 Aug 2022, Published Sep 2022

DOI: https://dx.doi.org/10.4314/tjs.v48i3.1

Abstract

High quality thin films are important for domain engineering applications such as on-volatile memory applications. Single crystalline (001) oriented Pb $(Zr_{0.5}T_{0.5})O_3$ thin films have been grown by pulsed laser deposition on $PrScO_3$ with strontium ruthenate (SRO) electrodes. Thin films were prepared from PZT ceramic targets with 15% excess PbO to compensate for lead loss at high deposition temperature. Layer by layer/step flow growth mode observed on AFM images has been realised by using a single terminated $PrScO_3$ substrate as well as optimized deposition parameters. XRD measurements have confirmed the highly (001) oriented tetragonal symmetry. Furthermore, analysis conducted using piezoresponse force microscopy has shown that the thin films are monodomain with spontaneous ferroelectric polarization preferentially pointing upwards, i.e., away from the substrate. The absence of ferroelastic domains and the observed single ferroelectric domain structure are the results of both relatively small compressive misfit strain as well as favourable electrical boundary conditions.

Keywords: PZT, Pulsed Laser Deposition, Epitaxy, Thin film.

Introduction

Lead Zirconate Titanate (PZT) belongs to the group of materials called piezoelectric ceramics. PZT is the most widely used piezoelectric ceramic in sensors, actuators, transducers and energy conversion applications because of its high electromechanical properties (Damjanovic 1998). PZT is a solid solution of $PbTiO_3$ (PTO) and $PbZrO_3$(PZO) compound and is denoted by $Pb(Zr_{1-x}Ti_x)O_3$. The phase boundary between the tetragonal and rhombohedral phases which is nearly independent of temperature is known as the *morphotropic phase boundary* (MPB), whose composition is $x = 0.48$. MPB is known for its uniquely high electromechanical properties (Jaffe et al. 1971, Damjanovic 1998, Setter 2002, Izyumskaya et al. 2007). A number of studies have reported the Pulsed Lased Deposition (PLD) growth of PZT thin films with different compositions especially at the morphotropic phase boundary (MPB) (Zhu et al. 2005, Zhu et al. 2006). However, these studies have reported only textured thin films, that is, thin films that are not single crystalline because of the high misfit strain between the thin film and amorphous TiN buffered Si(100) substrates used (Tagantsev et al. 2010).

Notably, the recently increasing interest in controlling other thin film properties such as those involving domain engineering for non-volatile memory devices has resulted in the exploration of the possibilities of growing thin films with controlled mechanical and

electrical boundary conditions (Tagantsev et al. 2010, Nataf et al. 2020). Achieving these goals requires the growth of epitaxial monocrystalline thin films. In this work, the PLD growth of single-crystalline Pb $(Zr_{0.5}T_{0.5})O_3$ (PZT 50/50) whose composition is close to MPB is reported. Thin film epitaxy is measured in terms of lattice misfit strain, which is given by:

$$u = \frac{a_s - a_f}{a_f} \qquad (1)$$

where a_s and a_f are the in-plane lattice parameters of the substrate and the thin film, respectively (Ohring 2001, Saghayezhian et al. 2021). If both the thin film and substrate are of the same material, the misfit strain is zero (homoepitaxy). Conventionally, for dissimilar materials (heteroepitaxy) the misfit strain is taken as positive for tensile strain and negative for compressive strain. It should be noted that both the thin film morphology and domain structure can be influenced by the nature and amount of misfit strain as well as processing technique. Too high misfit strain my results in either in-plain ferroelectric domains or the formation of ferroelastic domains or/and dislocations as a mechanism of thin film relaxation (Tagantsev et al. 2010). In this work, the growth of high-quality single crystalline thin films was achieved due to proper selection of the substrate, $PrScO_3$ (PSO), which imposes significantly low misfit strain as well as optimization of processing conditions.

Materials and Methods

PLD target preparation

PZT 50/50 ceramic target was prepared by using the same procedures used to process bulk PZT ceramics (Jaffe et al. 1971, Moulson and Herbert 2003), namely powder weighing and mixing, calcination and sintering.

(i) Powder mixing

Commercially available powder oxides listed in Table 1 were mixed to obtain 100 g of powders mixture at composition $Pb_{1.15}(Zr_{0.5}Ti_{0.5})O_3$, together with 75 ml isopropanol and 300 cylindrical ZrO_2 milling balls; and then milled by a planetary milling machine for 8 hours. After milling, isopropanol was then dried out by heating the mixture in a beaker with a hot plate and finally, the powder was separated from the milling balls by sieving.

(ii) Calcination process

After proper mixing, calcination of the powder mixture was done to ensure that chemical reactions take place between the mixed oxides to obtain the required compound. The calcination process also improves mixing by enabling initial interdiffusion of constituents to minimize the amount of diffusion that must take place during sintering in order to obtain PZT targets with homogeneous composition. The powder was sealed in alumina crucibles to minimize lead evaporation and then calcined as per conditions shown in Figure 1(a). Afterwards, the powder was milled again for further mixing using the same procedure as explained above.

(iii) Sintering process

Before sintering, the powders mixture was mixed with a 5% polyvinyl alcohol (PVA) water solution (made from 95% water and 5% PVA). PVA is used as a binder to increase the plasticity of the compacted powder and thus prevent cracking during dry pressing and sintering. Thereafter, cylindrical pellets with 30 mm diameter and 5 mm thickness were dry-pressed and embedded into the powder of similar composition in a crucible ready for sintering.

Table 1: Oxide powders used in the synthesis of PLD targets

Powder oxide	Purity [%]	Particle size [μm]	Supplier
Lead oxide (PbO)	99.99	4.78	Sigma-Aldrich GmbH
Zirconium dioxide (ZrO_2)	99.996	0.73	Tosoh Corporation
Titanium dioxide (TiO_2)	99.8	0.95	Alfa Aesar GmbH

Sintering was done in an electric furnace in two stages as shown in Figure 1. Stage one shown in Figure 1(b) involved burning out of the binder whereby the alumina crucible was not sealed by alumina to allow PVA evaporation. After the crucible had cooled down to room temperature, an alumina paster was applied around the crucible to seal possible openings in order to minimize lead evaporation during high-temperature sintering. Then, stage two of the sintering process proceeded in two steps, the first one involved lower temperature heating to dry the alumina paste, and the second one was the actual sintering (Figure 1(c)).

Figure 1: Heat treatment profiles and parameters for calcination and sintering parameters. (a) Calcination, (b) Binder removal step before final sintering, and (c) Two-step sintering: the first step involves drying of alumina paste used to seal crucibles to minimize PbO loss and the second step is the high-temperature sintering.

Substrates selection and treatment

Since the pseudocubic lattice parameter of PZT 50/50 is approximately 4.03034 Å, $PrScO_3$ substrate with a pseudocubic lattice parameter of 4.013 Å has been selected due to a relatively low misfit strain of about 4.3 x 10^{-3}. The $PrScO_3$ substrate belongs to the family of complex oxides of stable rare-earth scandates ($REScO_3$) (Kleibeuker et al. 2010). Before treatment, these oxides are double terminated; with both PrO and ScO_2 terminations in the case of $PrScO_3$. Since the nature of thin film growth mode is also influenced by the nature of substrate surface termination (Biswas et al. 2011), PSO substrates were treated by modifying (adopting) the methodology proposed by Kleibeuker et al. (2010). (110) PSO substrate was treated by using the following procedure: (i) Annealing at 900 °C for 1 hour, (ii) Ultrasonic soaking in deionized (DI)-water for 30 minutes, (iii) Buffered Hydrofluoric acid (BHF) etching for 5 seconds, (iv)12 M sodium hydroxide (NaOH) etching for 45 minutes and (iv) Ultrasonic soaking in 1M NaOH etching for 30 minutes.

PLD technique

Pulsed laser deposition (PLD) is a physical vapour deposition technique in which short high-power laser pulses are used to evaporate materials from a target surface and deposit them on the substrate (Willmott and Huber 2000, Chrisey and Hubler 2003). Figure 2 shows a schematic of the PLD system. The deposition process takes place inside the vacuum chamber where both the target and substrate were placed. The target is normally placed on the rotating carouser, while the substrate is attached to the heating element. When passing through a set of optical components (lenses), an intense laser pulse stream from an external source is focused onto the target where it is partially absorbed. The absorbed electromagnetic energy is converted into electronic excitation and then into thermal, chemical and mechanical energy which results in the

formation of a supersonic jet of plume directed towards the substrate. The plume may consist of atoms, molecules, electrons, ions, clusters, micro-sized solid particles and molten globules. Thin film growth occurs when plume materials recondense on the substrate. The threshold power density for plume formation depends on the target material, morphology and laser characteristics (that is, pulse wavelength and duration). To obtain good quality thin films, deposition frequency (rate), laser energy, substrate temperature as well as substrate-target distance should be optimized. In this work, about 2 nm strontium ruthenate (SRO) bottom electrode was first grown at 2Hz, 100 mTorr and 650 °C with laser energy of 250 mJ/pulse, followed by PZT grown at 3Hz, 300 mTorr and 575 °C with laser energy of 200 mJ/pulse.

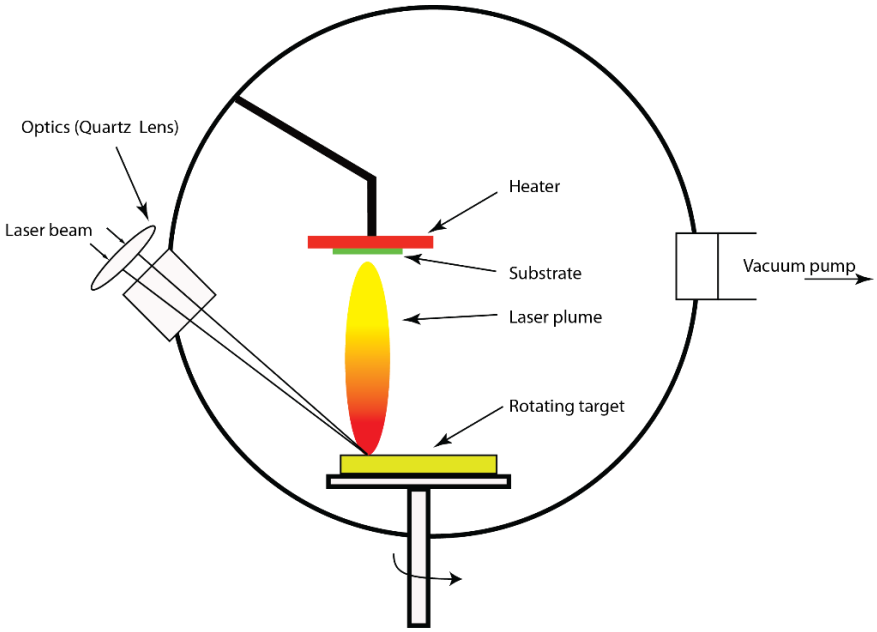

Figure 2: Schematic diagram of a PLD system.

Characterization techniques

Structural characterization of the processed thin films was done by both X-ray diffraction (XRD) and atomic force microscopy (AFM). XRD was used to identify crystalline phases, crystallographic orientations of the grown thin films as well as estimation of thin film thicknesses (Suryanarayana and Norton 1998). Imaging of the thin films' surface morphology was done by using AFM. Electrical characterization was done by using piezoresponse force microscopy (PFM). PFM utilizes the piezoelectric effect in imaging domain patterns in ferroelectric materials by employing the contact mode of AFM with alternating voltage on the tip (Gruverman et al. 2019, Asylum Research 2022). PFM measures the mechanical response when an alternating electrical voltage is applied to the sample surface with a conductive AFM tip according to Equation (2);

$$z = Z_{dc} + A\cos(\omega t + \varphi_{ph}) \qquad (2)$$

where z is the vertical surface deformation, Z_{dc} is displacement due to dc bias, A is the amplitude, $\omega = 2\pi f$ is the angular frequency of ac bias, f is the frequency and φ_{ph} is the phase. In response, the sample expands or contracts locally depending upon the local polarization direction as shown in Figure 3. The first harmonic component of the tip deflection determines the magnitude of the local piezoelectric response. The direction of the ferroelectric polarization below the tip is determined by the phase of the electromechanical response of the surface

relative to the tip voltage. PFM was thus used to establish the domain pattern of the as-grown thin films, i.e., single or multi-domain structure, as well as the preferential orientation of the ferroelectric polarization, i.e., either upwards, downwards or mixed. AFM and PFM imaging were carried out using an Asylum Research Cypher and Asyelec-01 Ti/Ir-coated silicon probes with a nominal force constant of 2 N/m and tip radius of 28 ± 10 nm.

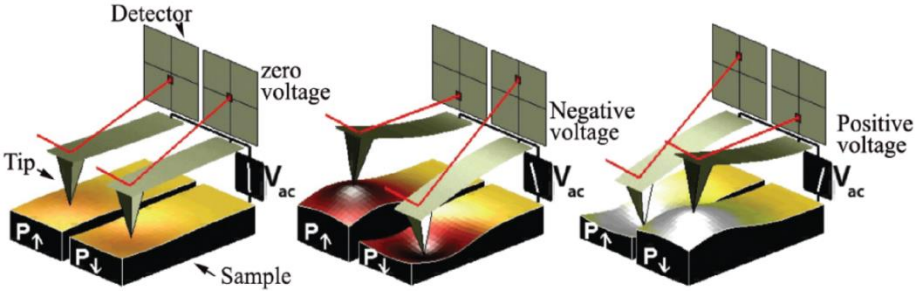

Figure 3: Schematic of PFM operation. The sample deforms in response to the applied voltage. The resulting cantilever deflection is detected and interpreted in terms of the domain patterns of the sample (Asylum Research 2022).

Results and Discussion

Substrate treatment

Controlled selective wet etching of complex oxide $PrScO_3$ resulted in ScO_2 terminated surface, similar to the results obtained on $DyScO_3$ (Kleibeuker et al. 2010). Figure 4 shows the (110) PSO substrate morphology after treatment, whereby the resulting atomic unit steps indicate that the selective etching process to obtain a single terminated surface was well achieved.

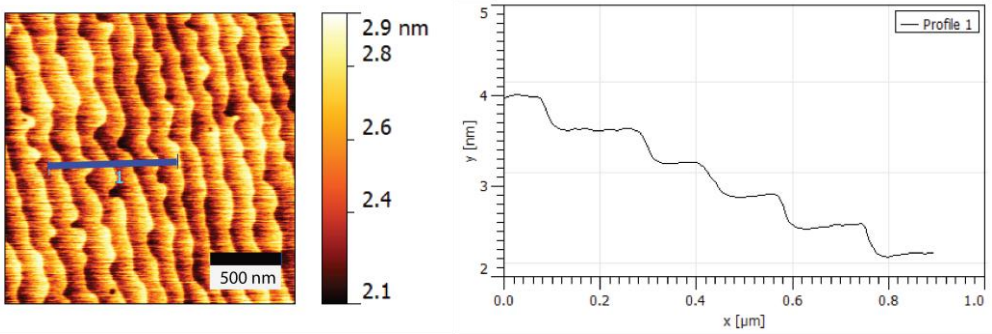

Figure 4: AFM image and surface profile of (110) PSO substrate after treatment.

Structural characterization of ceramic targets

The targets contained an excess of 15% mole-per cent Pb to compensate for lead volatility. The composition of the processed target was $Pb_{1.15}(Zr_{0.5}Ti_{0.5})O_3$, with a density of 7.53 g/cm^3 and a relative density of 0.94. The density value of the target is very close to the theoretical density of ceramics (8 g/cm^3) (Ochiai et al. 2008). The relative density was calculated based on stoichiometric ceramics and was used only to verify the solidity of the target.

XRD measurements were conducted to confirm the crystallographic phases of the targets before they are used in PLD. Figure 5 shows XRD patterns of PZT target compositions after sintering. Peaks were indexed by using PFD# 01-070-4057 (PZT) and PFD# 00-005-0561 (PbO) databases. It can be seen that PbO peaks are indicated by small triangles at (100) peaks.

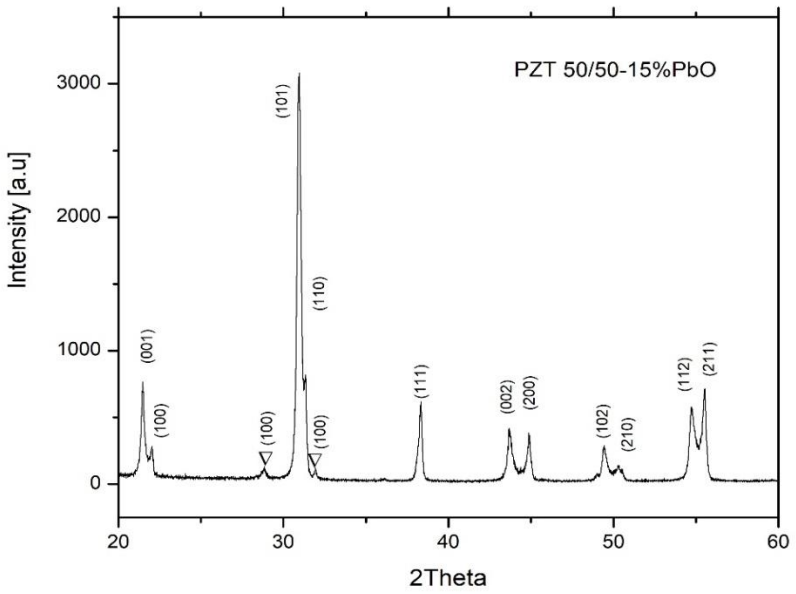

Figure 5: XRD pattern of PZT 50/50 target. PbO peaks are indicated by triangular symbols.

Structural characterization of thin films

The crystallographic phases and (001) orientation of PZT 30 nm PZT thin films were confirmed by using grazing incident XRD analysis as shown in Figure 6. The main figure shows (220) peaks for the PSO substrate, strained (002) PZT peak, and the (002) peak for the SRO bottom electrode. The insert shows an extended 2Theta scan up to 105°. The absence of any peaks for excess PbO indicates that there are no other second phases. Furthermore, the topography of both the bottom electrode (SRO) and the PZT thin films were determined by AFM. Figure 7 shows that both SRO and PZT thin films have a layer-by-layer/ step flow growth mode. The use of vicinal substrates whose surface morphology contains periodic patterns of terraces of singular faces and monatomic steps have induced step flow growth; whereby the step edges acted as defects where preferential nucleation occurred. In addition, steps heights act as diffusion barriers (Sangwal and Rodriguez-Clemente 1991). It should also be noted that the observed layer-by-layer growth suggests the two-dimensional misfit strain at the thin film-substrate interface is significantly low such that, the condition for the thin film relaxation through the formation of misfit dislocations was not met (Hu et al. 2003, Emelyanov and Pertsev 2003, Chu et al. 2004, Vrejoiu et al. 2006).

Electrical characterization of thin films

Piezoresponse force microscope (PFM) measurements were conducted on as-grown thin films to determine the structure of ferroelectric domains. The imaging was done on 2 µm x 2 µm regions at a scanning rate of 0.5 Hz and 256 lines. As can be seen in the vertical PFM images in Figure 7, the as-grown thin films showed no domain walls on the amplitude as well as no change of contrast in the phase image. This suggests that the as-grown thin films were monodomain. These results corroborate well with the tetragonal symmetry observed in the XRD measurements. The in-plane lattice parameters for the substrate and PZT thin film are 4.013 Å and 4.03034 Å, respectively (Mtebwa 2015). Using formula (1), the resulting compressive misfit strain imposed on the thin films can be estimated to be

0.43%. This significantly low value of misfit strain explains the absence of any ferroelastic domains in the PZT thin film (Tagantsev et al. 2010). Furthermore, it was noticed that the ferroelectric polarization of as-grown thin films had an upwards preferential direction, i.e., pointing away from the thin films-substrate interface. Similar observations have been reported for tetragonal $Pb(Zr_{0.2}TiO_{0.8})O_3$ composition grown on the SRO bottom electrode (Chen et al. 2013). This can be explained by the difference in work function between the substrate and electrode, resulting in the establishment of the built-in potential which manifests as band bending at the interface. In this particular case, the SRO work function (5.0 eV) (Scott et al. 1999) is smaller than that of PZT (5.8 eV) (Kumar and Niranjan 2014), and thus the downwards bending causes the spontaneous ferroelectric polarization to point upwards. To further confirm the preferential direction of the self-polarization, a positive 5 V d.c. was applied to the small region of 1.5 µm x 1.5 µm through an AFM tip in order to switch the polarization downwards. As shown in Figure 8, the switched region is in black contrast, indicating a successful 180° phase switching relative to the as-grown region.

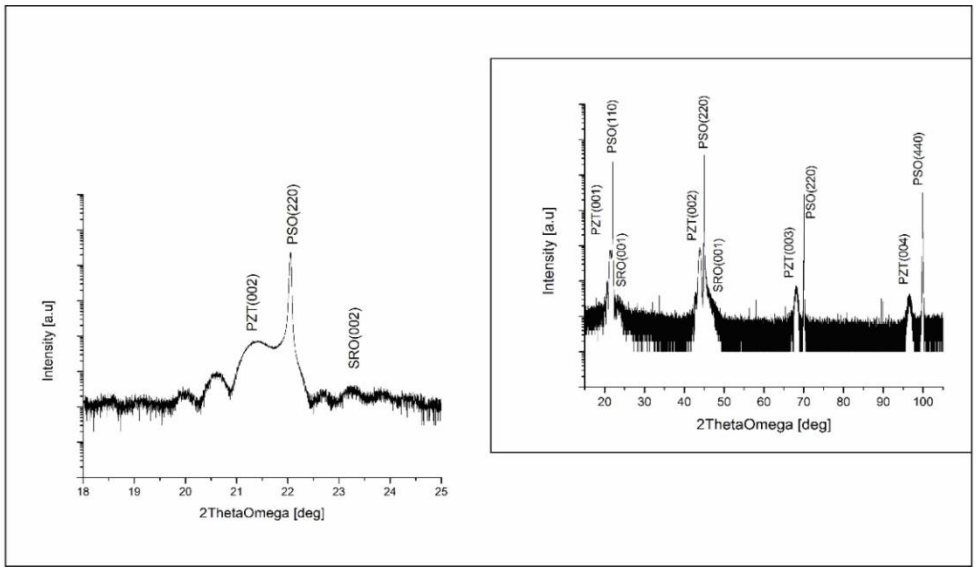

Figure 6: 2theta-Omega patterns for (002) peak of PZT 50/50 and SRO, and full scan pattern (insert).

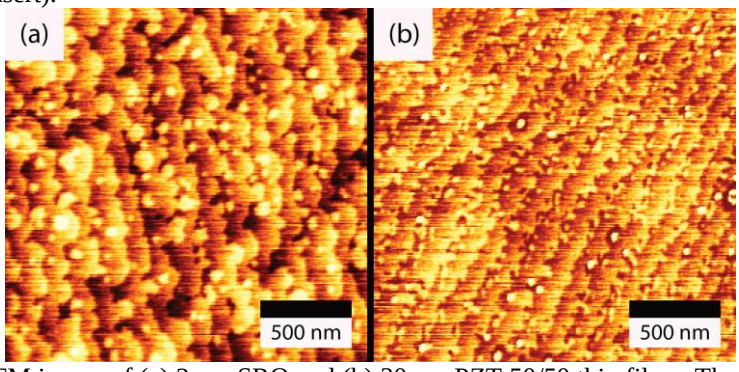

Figure 7: AFM image of (a) 2 nm SRO and (b) 30 nm PZT 50/50 thin films. The roughness of PZT and SRO are about 0.144 nm and 0.149 nm, respectively.

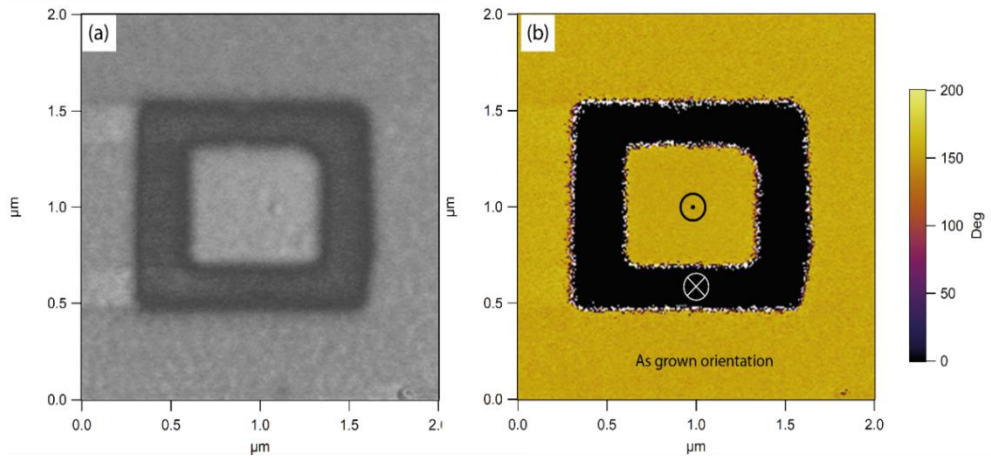

Figure 8: 30 nm thick PZT 50/50 with 15% excess PbO on SRO. (a) AFM (a) PFM Vertical amplitude and (c) PFM Vertical phase. As-grown thin film has an upward polarization direction. The switched bottom region was obtained by poling the sample with +5V dc bias on the AFM tip.

Conclusion

Defect-free single-crystalline PZT 50/50 thin film has been grown successfully with (001) orientation by pulsed laser deposition. These thin films have shown layer-by-layer step flow growth due to low lattice mismatch attained by choosing PSO substrate with (110) orientation. Moreover, the observed growth has also been contributed by the use of a single surface terminated substrate, which was achieved through optimized substrate treatment conditions. The use of PSO substrate has imposed a significantly low value of misfit strain of 0.43%, which in turn has resulted in a single domain, unrelaxed thin films without ferroelastic domains. The single domain tetragonal symmetry was further confirmed by the PFM measurements.

Acknowledgement

The author would like to thank the Swiss National Science Foundation for funding this project.

References

Asylum Research 2022 *Piezoresponse Force Microscopy with Asylum Research AFMs* [Online]. Asylum Research. Available: https://afm.oxinst.com/assets/uploads/products/asylum/documents/Piezoresponse-Force-Microscopy-AFM-web.pdf [Accessed 27-03- 2022].

Biswas A, Rossen PB, Yang CH, Siemons W, Jung MH, Yang IK, Ramesh R and Jeong YH 2011 Universal Ti-rich termination of atomically flat $SrTiO_3$ (001),(110), and (111) surfaces. *Appl. Phys. Lett.* 98: 051904.

Chen J, Lu H, Liu HJ, Chu YH, Dunn S, Ostrikov KK, Gruverman A and Valanoor N 2013 Interface control of surface photochemical reactivity in ultrathin epitaxial ferroelectric films. *Appl. Phys. Lett.* 102: 182904.

Chrisey DB and Hubler GK 2003 Pulsed laser deposition of thin films. In: *Chrisey DB, Hubler GK (Eds) Pulsed Laser Deposition of Thin Films,* pp. 648. ISBN 0-471-59218-8. Wiley-VCH.

Chu MW, Szafraniak I, Scholz R, Harnagea C, Hesse D, Alexe M and Gösele U 2004 Impact of misfit dislocations on the polarization instability of epitaxial nanostructured ferroelectric perovskites. *Nat. Mater.* 3: 87-90.

Damjanovic D 1998 Ferroelectric, dielectric and piezoelectric properties of ferroelectric thin films and ceramics. *Rep. Prog. Phys.* 61: 1267.

Emelyanov AY and Pertsev NA 2003 Abrupt changes and hysteretic behavior of 90°

domains in epitaxial ferroelectric thin films with misfit dislocations. *Phys. Rev. B* 68: 214103.

Gruverman A, Alexe M and Meier D 2019 Piezoresponse force microscopy and nanoferroic phenomena. *Nat. Commun.* 10: 1-9.

Hu S, Li Y and Chen L 2003 Effect of interfacial dislocations on ferroelectric phase stability and domain morphology in a thin film—A phase-field model. *J. Appl. Phys.* 94: 2542-2547.

Izyumskaya N, Alivov YI, Cho SJ, Morkoc H, Lee H and Kang YS 2007 Processing, structure, properties, and applications of PZT thin films. *Crit. Rev. Solid State Mater. Sci.* 32: 111-202.

Jaffe B, Cook WR and Jaffe H 1971 Piezoelectric Ceramics, Academic Press Inc.

Kleibeuker JE, Koster G, Siemons W, Dubbink D, Kuiper B, Blok JL, Yang C-H, Ravichandran J, Ramesh R, Ten Elshof JE and Others 2010 Atomically defined rare-Earth scandate crystal surfaces. *Adv. Funct. Mater.* 20: 3490-3496.

Kumar VS and Niranjan MK 2014 Effect of surface structure on workfunction and Schottky-barrier height in $SrRuO_3/SrTiO_3$ (001) heterojunctions. *J. Appl. Phys.* 115: 173705.

Moulson AJ and Herbert JM 2003 Electroceramics: materials, properties, applications, John Wiley & Sons.

Mtebwa M 2015 *Monocrystalline PZT thin films.* EPFL.

Nataf G, Guennou M, Gregg J, Meier D, Hlinka J, Salje E and Kreisel J 2020 Domain-wall engineering and topological defects in ferroelectric and ferroelastic materials. *Nat. Rev. Phys.* 2: 634-648.

Ochiai H, Hayano S, Shoji K, Kimura O and Maiwa H 2008 High-curie-temperature Pb (Zr, Ti) O_3 ceramic actuator cofired with pure silver internal electrodes. *Jpn. J. Appl. Phys.* 47: 5534.

Ohring M 2001 Materials science of thin films: depositon & structure, Elsevier.

Saghayezhian M, Wang Z, Howe D, Siwakoti P, Plummer EW, Zhu Y and Zhang J 2021 Formation of dislocations via misfit strain across interfaces in epitaxial $BaTiO_3$ and $SrIrO_3$ heterostructures. *J. Phys.: Condens. Matter* 33: 275003.

Sangwal K and Rodriguez-Clemente R 1991 Surface Morphology of Crystalline Materials, Sci-Tech Publications, Zürich.

Scott J, Watanabe K, Hartmann A and Lamb R 1999 Device models for PZT/Pt, BST/Pt, SBT/Pt, and SBT/Bi ferroelectric memories. *Ferroelectrics* 225: 83-90.

Setter N 2002 ABC of piezoelectric materials. In: Setter N (Ed). *Piezoelectric Materials in Devices: Extended Reviews on Current and Emerging Piezoelectric Materials, Technology, and Applications*. Ceramics Laboratory, EPFL Swiss Federal Institute of Technology.

Suryanarayana C and Norton MG 1998 X-ray diffraction: a practical approach, Springer.

Tagantsev AK, Cross LE and Fousek J 2010 Domains in ferroic crystals and thin films, Springer, New York.

Vrejoiu I, Le Rhun G, Pintilie L, Hesse D, Alexe M and Gösele U 2006 Intrinsic ferroelectric properties of strained tetragonal $PbZr_{0.2}Ti_{0.8}O_3$ obtained on layer-by-layer grown, defect-free single-crystalline films. *Adv. Mater.* 18: 1657-1661.

Willmott PR and Huber JR 2000 Pulsed laser vaporization and deposition. *Rev. Mod. Phys.* 72: 315.

Zhu T, Lu L and Lai M 2006 Growth and electrical properties of highly (0 0 1)-oriented Pb ($Zr_{0.52}Ti_{0.48}$) O_3 thin films on amorphous TiN buffered Si (1 0 0). *Sensors and Actuators A: Physical* 125: 335-339.

Zhu TJ, Lu L and Lai MO 2005 Pulsed laser deposition of lead-zirconate-titanate thin films and multilayered heterostructures. *Appl. Phys. A* 81: 701-714.